Adv. Polar Upper Atmos. Res., **19**, 63–70, 2005

Research note

Relationship between thermospheric vertical wind and the location of ionospheric current in the polar region

Mamoru Ishii

National Institute of Information and Communications Technology, Koganei-shi, Tokyo 184-8795
E-mail: mishii@nict.go.jp

(Received November 5, 2004; Accepted January 25, 2005)

Abstract: We have been observing vertical winds in the polar thermosphere with a Fabry-Perot interferometer (FPI) installed at Poker Flat Research Range, Alaska. To introduce a new method to understand thermospheric wind system in the polar region, the vertical wind variations are compared with the peak location of ionospheric current deduced from magnetic field measurements on the ground in a case observed on December 5, 1999. The magnetometer data were obtained at Kaktovik, Fort Yukon, Poker Flat, and Gakona. The method of estimating ionospheric current was obtained from H. Lühr *et al.* (J. Atmos. Terr. Phys., **56**, 81, 1994). The eastward current dominant interval was clearly separated from the westward current dominant one at 1130 UT (~0030 MLT) in this case. The relation between the vertical wind and the location of the ionospheric current was clearly different before and after the boundary. Namely, the downward (upward) vertical wind was found to be dominant equatorward (poleward) of the ionospheric current after 1130 UT, which is consistent with results obtained in many previous works. However, this relation was found to be opposite before 1130 UT: the upward (downward) vertical wind was seen to be equatorward (poleward) of current.

key words: vertical wind, thermosphere-ionosphere coupling, ionospheric current, Fabry-Perot Interferometer, magnetometer

1. Introduction

Since large vertical winds have been found near the auroral zone with Fabry-Perot interferometers (FPIs; Rees *et al.*, 1984), many studies focused attention on the phenomenon (Crickmore *et al.*, 1991; Price and Jacka, 1991; Conde and Dyson, 1995; Aruliah and Rees, 1995; Smith and Hernandez, 1995; Price *et al.*, 1995; Innis *et al.*, 1996, 1997; Ishii *et al.*, 1999, 2001). These vertical winds play a significant role in determining the composition, large scale circulation and energy balance of the upper atmosphere. Several sources are considered to generate such large vertical winds; (1) Joule and particle heating, (2) divergence and convergence of horizontal winds, and (3) gravity waves propagating from the lower atmosphere. Joule heating is one of the most likely sources of the vertical winds in the polar thermosphere. Although a number of

studies have been conducted on this subject, there have been few studies that discuss the relationship between lower thermospheric vertical wind and ionospheric current, which is the source of Joule heating (Rees *et al.*, 1984; Peteherych *et al.*, 1985).

In this study, we estimate temporal variation of the ionospheric current peak using the Alaskan magnetometer chain, and research the relation between the deduced current peak and the vertical winds in the lower thermosphere. The typical height of OI 557.7 nm emission layer is 110–140 km which is close to the peak height of ionospheric current and appropriate to discuss the effect of current to neutral wind. The method shown in Lühr *et al.* (1994) was used for estimating the current peak. Some of the previous studies have stated that the direction of vertical wind depends on the relative location of the auroral oval (Innis *et al.*, 1996, 1997; Crickmore *et al.*, 1991). However, most studies deduced the location of the oval from optical measurements on the ground, and it has not been confirmed whether the observed boundary is the real one between open and closed magnetic field lines.

The first motivation for the paper is to investigate the vertical wind system on the vicinity of ionospheric current, instead of optical aurora. In our method, the location of the dominant ionospheric current can be estimated without auroral images. This paper introduces this new method for discussing the relation between Joule heating and vertical wind, and shows an initial result obtained in a case study measured on December 5, 1999.

Some analysis of magnetometer data corresponding to thermospheric vertical wind events were reported in Innis *et al.* (1996). They had a spectral analysis of fluxgate magnetometer data obtained at Mawson on the nights when significant periodicities were seen in the FPI data. The vertical component of the magnetic field exhibited evidence of a correlation with the wind data, where an interval of upward wind was likely to be associated with an interval of increased upward field strength.

We need many of the information such as electric field, ionospheric conductivity and horizontal component of neutral winds to understand completely the neutral wind system in the polar thermosphere including vertical winds. For these, several additional observations are required such as incoherent scatter radar, HF radar and Doppler Imaging FPI. This paper will be placed as a small but practical step toward these simultaneous observations, with showing that the magnetometer data also gives us important information.

2. Instrumentation and observations

The Communications Research Laboratory FPI (CRLFPI) project operates two types of FPIs, one with a narrow field of view and the other with a wide field of view (details of these instruments were described in Ishii *et al.*, 1997). The narrow field-of-view FPI (scanning FPI) was installed at Poker Flat, Alaska in September 1998. A single, 116 mm aperture etalon with servo-control of the etalon spacing is operated at a 20.49 mm gap. The field of view is 1.4 deg full-angle and is fixed to the zenith direction. Each fringe pattern image of the λ630.0 nm and λ557.7 nm emissions of atomic oxygen are recorded simultaneously on each of two output channels every 2 min. Each image has 3 orders of interference for 630.0 nm and 4 order for 557.7 nm at the etalon. We use two kinds of laser for calibration; a He-Ne green laser (543.5 nm) for the shorter

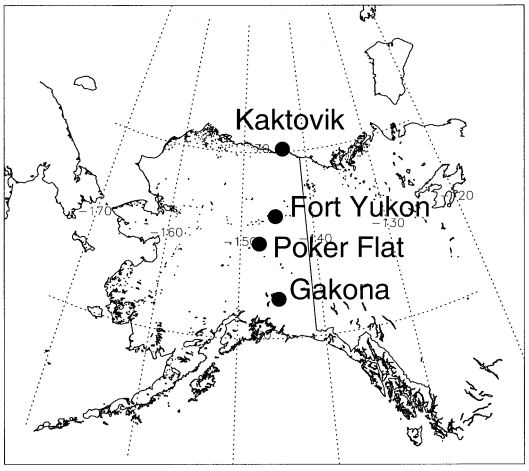

Fig. 1. Location of the observatories. The CRLFPI was operated at Poker Flat Research Range. The magnetic field was measured at Fort Yukon, Gakona, and Poker Flat. This map is plotted with geographic coordinates.

wavelength and a frequency-stabilized He-Ne red laser for the longer wavelength. We obtain one laser image per every ten observations (every~20 min), which allows us to characterize and correct for the effect of etalon gap drift. Wind velocities deduced from both channel images are also calibrated with the same frequency-stabilized laser.

A one-night average of vertical wind measurement was used to determine the zero Doppler shift, keeping in mind the possibility of constant offset in wind velocity. Another study using the same system shows high correlation over 0.7 between the wind velocity variations obtained two independent FPIs 300 km distant from each other along auroral arc (Ishii *et al.*, 2004). This result will be an evidence that our baseline determination is acceptable.

The magnetometer used here (The Geophysical Institute Magnetometer Array) has a basic fluxgate design using a triaxial set of cores (Narod ring-core magnetometer, Narod Geophysics Lt., Canada). Figure 1 shows the location of the four observatories at which the geomagnetic field was recorded; Poker Flat (65.12 N, 147.43 W), Kaktovik (70.16 N, 143.67 W), Gakona (62.12 N, 145.14 W) and Fort Yukon (66.56 N, 145.22 W). The magnetometer electronics are controlled by an S-100 computer that uses internal calibrations to produce digital output in units of nano-Tesla. The nominal data rate is 8 samples per second and 1 s-average data were obtained for this study. The temperature instability of the sensor is less than 0.1 nT/degree and the long-term drift is less than 10 pT/day. The noise level is $7\,\mathrm{pT}/\sqrt{Hz}$ at 1 Hz. The error in orthogonality is less than 0.1 degrees.

3. Method of analysis and results

We adopted the method described in Lühr *et al.* (1994) for deducing the ionospheric current distribution. We assumed a single, magnetic east-west ionospheric

current with Gaussian-shape distribution as the first approximation, following Lühr *et al.* (1994). The ΔH-components of magnetometer data at four sites were used to determine three parameters: peak location, height and width. Since four-point data of the magnetic field did not provide enough information to determine the peak of ionospheric current with Gaussian-fitting in many cases, the magnitude of the ΔH-component at infinite North and South was assumed to be zero. The baseline of magnetic field variation was calculated from the averaged value over five quiet days for each observatory. Zonal direction of the ionospheric current was deduced from the signature of the height of the fitting Gaussian (positive: eastward).

Figure 2 shows the result obtained on December 5, 1999. The top panel shows auroral luminosity with OI 557.7 nm fringes. The solid and dotted lines show the intensities at the maximum and minimum counts in the inner fringe data. The

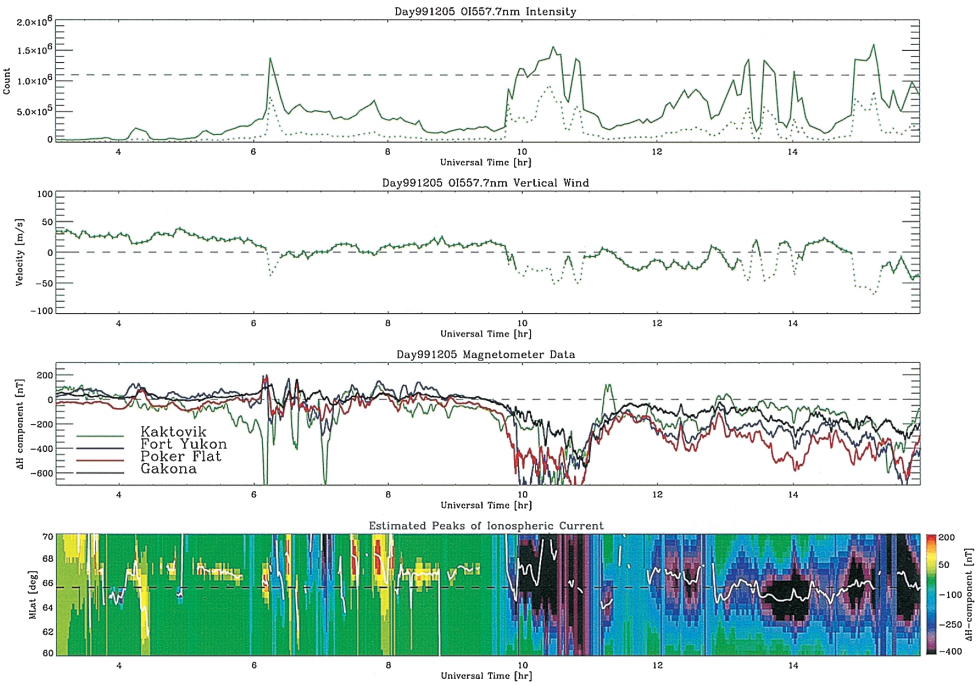

Fig. 2. The result of comparison between the vertical wind and the location of ionospheric current deduced from December 5, 1999 observation. Top panel: auroral luminosity with OI557.7 nm fringes. The solid and dotted lines show the intensities at the top and bottom of the innermost fringe. Second panel: vertical winds estimated from OI557.7 nm emission (upward positive). When the fringe is saturated with bright aurora ($>1.10\times10^6$ count), it is shown by a dotted line. Third panel: the ΔH-component of magnetic field perturbations. Results were obtained at Kaktovik (green), Fort Yukon (blue), Poker Flat (red), and Gakona (black). Bottom panel: "estimated peaks of ionospheric currents." The vertical axis shows latitudinal distribution of ionospheric currents assuming single Gaussian distribution. The broken line shows the latitude of PFRR, in which the vertical winds were measured. White lines in this panel show the peak location of ionospheric currents.

magnetic midnight corresponds to ~1100 UT. The second panel shows vertical winds in the OI 557.7 nm emission layer whose altitude is generally ~110 km (*e.g.*, Shepherd *et al.*, 1995). The upward velocity shows a positive signature. Ishii *et al.* (2001) show the detailed method of analysis to obtain the vertical winds. When the observed aurora was too bright, the recorded fringes saturate; this can lead to overestimation of temperature and large errors in velocity. The maximum count in two minutes was 1.206×10^6 and we show wind velocity with a dotted line when the peaks of fringe images had a count of greater than 1.10×10^6. The third panel shows ΔH-components of magnetometer data at four sites, subtracted the average of five quiet days as baselines. The fourth panel shows estimated peaks of ionospheric current, with the vertical axis showing latitudinal distribution of ionospheric currents assuming single Gaussian distribution. The equivalent current was used in this study which is proportional to the variation of magnetic field on the ground: the unit is nT. The color code in the forth panel shows equivalent current (or estimated distribution of ΔH-components of magnetic field) along the magnetic latitude. The broken line shows the latitude of the Poker Flat Research Range (PFRR), which the vertical winds were measured. The white lines in the panel show the location of estimated peaks of ionospheric currents.

Figure 3 is given as an aid for discussing the relation between vertical wind and the

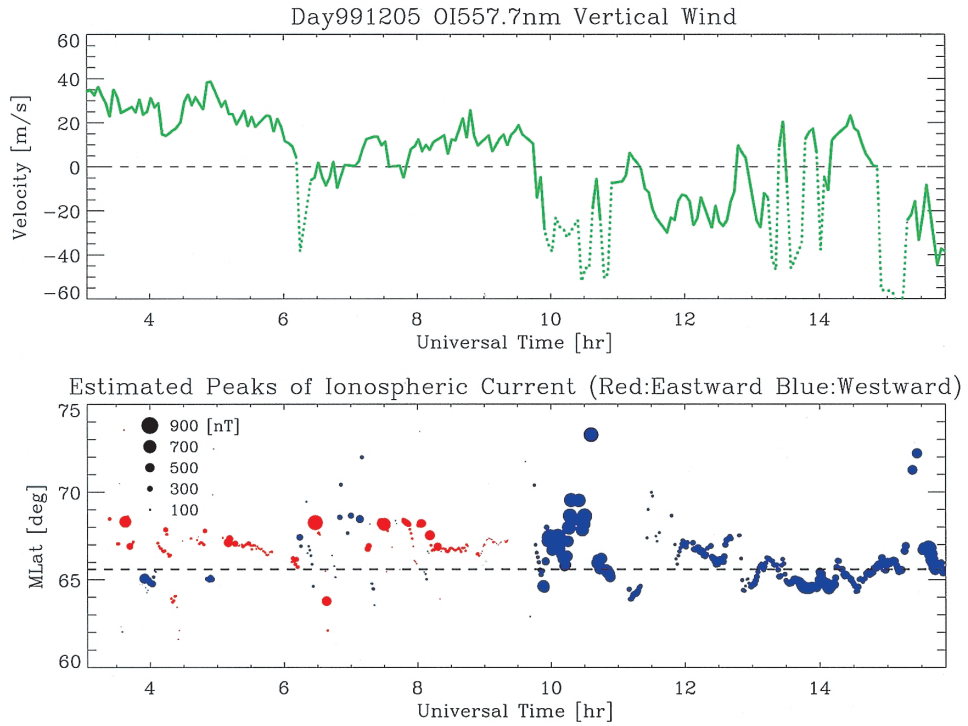

Fig. 3. Top panel: the same as the second panel of Fig. 2. Bottom panel: the location of estimated peaks of ionospheric currents. The size and color of circles show the current magnitude and the direction of the current (red: eastward, blue: westward).

location and direction of ionospheric currents. The top panel of the figure is the same as the second panel of Fig. 2. The bottom panel shows the location of estimated peaks of ionospheric currents. The size of the points shows the current magnitude and the color shows the direction of the currents (red: Eastward, blue: Westward). This panel shows a boundary at around 0930 UT; eastward currents existed only before the boundary. The relation between the vertical wind and the location of ionospheric currents changed both before and after the boundary. Namely, before 0930 UT, there was a relatively eastward current poleward of PFRR that was dominant. During this period the vertical wind flowed upward.

The magnetic field was considerably disturbed from 1000 to 1100 UT. During this interval there was a strong westward current poleward of PFRR and the vertical wind accelerated downward strongly (It should be noted that the absolute value of wind velocity is not accurate in this interval because of fringe saturation with bright aurora). Just after 1100 UT a weak westward current was detected when upward acceleration was observed in the vertical wind. After this event the current was poleward of PFRR, and the vertical wind kept flowing downward until 1300 UT. There was some fluctuation from 1300 to 1500 UT, but generally the current reached the equatorwardmost location at 1400 UT and then moved poleward again. The vertical wind variation showed the different tendency from the previous interval, namely, when the current located poleward (equatorward) of PFRR, downward (upward) vertical wind was generally observed.

4. Discussions

The main purpose of this paper is to introduce a method to estimate the location of ionospheric currents for understanding vertical winds in the thermosphere, rather than to show new results. It should be noted that it is impossible to conclude that the results are general or special for this case because of one case study.

The most notable point in the results we obtained is that upward wind was observed equatorward of ionospheric currents (and optical aurora) before 0930 UT. Most of the previous works show an upward (downward) wind poleward (equatorward) of the auroral oval (Crickmore *et al.*, 1991; Price *et al.*, 1995; Innis *et al.*, 1996, 1997; Ishii *et al.*, 2001). The vertical wind configuration observed on the morning side (*i.e.*, after magnetic midnight at 1100 UT) in the present observation is consistent with these results, but on the evening side is opposite to them. Although no relationships, even casual ones, have yet been found between the two, this upward wind region corresponds to the eastward current region.

Innis *et al.* (1996) reported a relationship between the magnetometer data and OI630.0 nm vertical wind found from a cross correlation at Mawson. The results appear to be consistent with the 'morning regime' identified in our results.

We consider two possible ways that these wind patterns may be built, both upward on the equator side of aurora in the pre-midnight sector and the opposite relation between vertical wind and aurora in the post-midnight sector. The first of these is variation of the ionospheric current source in the auroral oval. Kamide (1988) shows schematic distribution of electric field/conductivity dominant regions. The Harang

discontinuity is clearly manifested as a switch from the eastward to the westward electrojet, and more specifically as a switch from the "electric field" dominant electrojet to the "conductivity" dominant electrojet. There is another boundary in the morning sector that divides the electric field/conductivity dominant region (Fig. 9.6 in Kamide's paper). Because the ionospheric Joule heating rate is proportional to conductivity and the square of the electric field, the neutral gas is heated more effectively in the electric field dominant region than in the conductivity dominant region. The electric field dominant region shown in Kamide (1988) is equatorward of the oval in the pre-midnight region, and poleward of the oval in the post-midnight region; the Joule heating rate can be stronger in the region than in others.

Second, Lorentz force may contribute to the building of the wind patterns. A similar idea is discussed in Peteherych *et al.* (1985). They mentioned that $J \times B$ force is downward (upward) when the westward (eastward) electrojets are observed. This idea sounds persuasive because our case shows that the direction of the ionospheric current are opposite to each other where the relation between vertical wind and the location of aurora is opposite: the correlation between vertical wind and estimated peaks of ionospheric current is positive (negative) during the eastward (westward) current was observed (Fig. 3). In this case, the direction of Lorentz force is perpendicular to the magnetic field and the inclination of the magnetic field is 77.49 deg at PFRR. This means that if the observed vertical wind was driven by Lorentz force, there should be a horizontal wind about 4.5 times (~tan 77.49) larger than the vertical winds. However, our results shows more complicated relation between ionospheric currents and the vertical winds: vertical wind velocity varied significantly even when the current direction did not change. It means that we need any other mechanism to explain the phenomena, even if the Lorentz force may be one of the sources of the vertical winds.

5. Concluding remarks

The temporal variation of vertical winds in the polar thermosphere deduced from OI557.7 nm observation with an FPI was compared with the location and intensity of the ionospheric current estimated from geomagnetic field data obtained from Alaska chain observatories. A case study observed on December 5, 1999 was presented in this study.

The eastward current dominant interval was clearly separated from the westward current dominant one at 1130 UT in this case. The relation between the vertical wind and the location of ionospheric current between before and after the boundary was clearly different. Namely, the downward (upward) vertical wind was found to be dominant equatorward (poleward) of the ionospheric current after 1130 UT (~0030 UT), which is consistent results obtained in many previous works. Before this time, however, the opposite relation held. This difference may be explained by the MLT dependence of effective Joule heating rate and/or Lorentz force driving, but more observational results will be required before this can be ascertained with precision.

Acknowledgments

The magnetometer data was provided by John Olson, Geophysical Institute,

University of Alaska, Fairbanks. We thank June Pelehowski and Brian Lawson for supporting the operation of the Fabry-Perot interferometers, Meridian Scanning Photometer, and the observatory at Poker Flat. This study has been supported in part by the U.S.-Japan International Research Project to observe the middle atmosphere, NICT.

The editor thanks Dr. J. L. Innis and another referee for their help in evaluating this paper.

References

Aruliah, A.L. and Rees, D. (1995): The trouble with thermospheric vertical winds: geomagnetic, seasonal and solar cycle dependence at high latitudes. J. Atmos. Terr. Phys., **57**, 597–609.

Conde, M. and Dyson, P. (1995): Thermospheric vertical winds above Mawson, Antarctica. J. Atmos. Terr. Phys., **57**, 589–596.

Crickmore, R.I., Dudeney, J.R. and Rodger, A.S. (1991): Vertical thermospheric winds at the equatorward edge of the auroral oval. J. Atmos. Terr. Phys., **53**, 485–492.

Innis, J.L., Greet, P.A. and Dyson, P.L. (1996): Fabry-Perot spectrometer observations of the auroral oval/polar cap boundary above Mawson, Antarctica. J. Atmos. Terr. Phys., **58**, 1973–1988.

Innis, J.L., Dyson, P.L. and Greet, P.A. (1997): Further observations of the thermospheric vertical wind at the auroral oval/polar cap boundary above Mawson station, Antarctica. J. Atmos. Terr. Phys., **59**, 2009–2022.

Ishii, M., Okano, S., Sagawa, E., Watari, S., Mori, H., Iwamoto, I. and Murayama, Y. (1997): Development of Fabry-Perot interferometers for airglow observations. Proc. NIPR Symp. Upper Atmos. Phys., **10**, 97–108.

Ishii, M., Oyama, S., Nozawa, S., Fujii, R., Sagawa, E., Watari, S. and Shinagawa, H. (1999): Dynamics of neutral wind in the polar region observed with two Fabry-Perot Interferometers. Earth Planets Space, **51**, 833–844.

Ishii, M., Conde, M., Smith, R.W., Krynicki, M., Sagawa, E. and Watari, S. (2001): Vertical wind observations with two Fabry-Perot interferometers at Poker Flat, Alaska. J. Geophys. Res., **106**, 10537–10551.

Ishii, M., Kubota, M., Conde, M., Smith, R.W. and Krynicki, M. (2004): Vertical wind distribution in the polar thermosphere during Horizontal E Region Experiment (HEX) campaign. J. Geophys. Res., **109**, doi: 10.1029/2004JA010657.

Kamide, Y. (1988): Electrodynamic Processes in the Earth's Ionosphere and Magnetosphere. Kyoto, Kyoto Sangyo Univ. Press, 756 p.

Lühr, H., Geisler, H. and Schlegel, K. (1994): Current density models of the eastward electrojet derived from ground-based magnetic field and radar measurements. J. Atmos. Terr. Phys., **56**, 81–91.

Peteherych, S., Shepherd, G.G. and Walker, J.K. (1985): Observation of vertical E-region neutral winds in two intense auroral arcs. Planet. Space Sci., **33**, 869–873.

Price, G.D. and Jacka, F. (1991): The influence of geomagnetic activity on the upper mesosphere/lower thermosphere in the auroral zone. I. Vertical winds. J. Atmos. Terr. Phys., **53**, 909–922.

Price, G.D., Smith, R.W. and Hernandez, G. (1995): Simultaneous measurements of large vertical winds in the upper and lower thermosphere. J. Atmos. Terr. Phys., **57**, 631–643.

Rees, D., Smith, R.W., Charleton, P.J., McCormac, F.G., Lloyd, N. and Steen, A. (1984): The generation of vertical winds and gravity waves at auroral latitudes -I. Observations of vertical winds. Planet. Space Sci., **38**, 667–684.

Shepherd, G.G., Thuillier, G., Solheim, B.H., Rochon, Y.J., Criswick, J., Gault, W.A., Peterson, R.N., Wiens, R.H. and Zhang, S.-P. (1995): WINDII on UARS—Status report and preliminary results. The Upper Mesosphere and Lower Thermosphere, ed. by R.M. Johnson and T.L. Killeen. Washington, D.C., Am. Geophys. Union, 297–304 (Geophysical Monograph **87**).

Smith, R.W. and Hernandez, G. (1995): Vertical winds in the thermosphere within the polar cap. J. Atmos. Terr. Phys., **57**, 611–620.